FEBS Open Bio 4 (2014) 672–682

FEBS openbio

journal homepage: www.elsevier.com/locate/febsopenbio

# Adenylate kinase from *Streptococcus pneumoniae* is essential for growth through its catalytic activity

Trung Thanh Thach [a,1], Truc Thanh Luong [b,1], Sangho Lee [a,*], Dong-Kwon Rhee [b,*]

[a] Department of Biological Sciences, Sungkyunkwan University, Suwon 440-746, Republic of Korea
[b] School of Pharmacy, Sungkyunkwan University, Suwon 440-746, Republic of Korea

ARTICLE INFO

*Article history:*
Received 6 May 2014
Revised 26 June 2014
Accepted 2 July 2014

*Keywords:*
*Streptococcus pneumoniae*
Adenylate kinase
Crystal structure
Bacteria growth
Virulence factor

ABSTRACT

***Streptococcus pneumoniae*** **(pneumococcus) infection causes more than 1.6 million deaths worldwide. Pneumococcal growth is a prerequisite for its virulence and requires an appropriate supply of cellular energy. Adenylate kinases constitute a major family of enzymes that regulate cellular ATP levels. Some bacterial adenylate kinases (AdKs) are known to be critical for growth, but the physiological effects of AdKs in pneumococci have been poorly understood at the molecular level. Here, by crystallographic and functional studies, we report that the catalytic activity of adenylate kinase from *S. pneumoniae* (SpAdK) serotype 2 D39 is essential for growth. We determined the crystal structure of SpAdK in two conformations: ligand-free open form and closed in complex with a two-substrate mimic inhibitor adenosine pentaphosphate (Ap5A). Crystallographic analysis of SpAdK reveals Arg-89 as a key active site residue. We generated a conditional expression mutant of pneumococcus in which the expression of the *adk* gene is tightly regulated by fucose. The expression level of *adk* correlates with growth rate. Expression of the wild-type *adk* gene in fucose-inducible strains rescued a growth defect, but expression of the Arg-89 mutation did not. SpAdK increased total cellular ATP levels. Furthermore, lack of functional SpAdK caused a growth defect *in vivo*. Taken together, our results demonstrate that SpAdK is essential for pneumococcal growth *in vitro* and *in vivo*.**

© 2014 The Authors. Published by Elsevier B.V. on behalf of the Federation of European Biochemical Societies. This is an open access article under the CC BY-NC-ND license (http://creativecommons.org/licenses/by-nc-nd/3.0/).

## 1. Introduction

*Streptococcus pneumoniae* (the pneumococcus), an encapsulated Gram-positive, causes life-threatening infections (pneumonia, bacteremia, meningitis), and claims more than 1.6 million deaths worldwide per year [1]. Streptococcal virulence is mediated by many cell-surface virulence factors including capsular polysaccharides and proteins as well as intracellular pneumolysin [2]. Nevertheless, survival and growth of pneumococci are prerequisites for virulence.

ATP is involved in many cellular metabolic processes as a major energy source, and could be a modulating factor for virulence [3]. Availability of the energy levels to living cells is dictated by adenine nucleotide homeostasis. Thus, rigorous control of adenine nucleotide homeostasis is crucial to cellular metabolism. Adenylate energy charge (EC) in living cells is definded as follows [4]:

$$EC = [ATP] + 0.5\frac{[ADP]}{[AMP] + [ADP] + [ATP]}$$

EC is the amount of energy readily accessible for cellular metabolism [4,5] that may affect other fundamental pathogenesis such as bacterial growth, virulence factors, and secretion pathways [6,7].

Adenylate kinase (AdK; ATP:AMP phosphotransferase; EC 2.7.4.3) catalyzes conversion between adenylate nucleotides [8]: Mg. ATP + AMP ↔ Mg. ADP + ADP. AdK has been attributed to the synthesis and maintenance of adenine nucleotide homeostasis, which is crucial in cellular viability and cell energy [8]. In *Escherichia coli*, AdK is essential to cellular growth and survival, for regulation of adenine nucleotide homeostasis [9]. However, it has remained elusive as to whether AdK is essential in Gram-positive bacteria. To explore the possibility that AdK from *S. pneumoniae* (SpAdK) is crucial in pneumococcal growth by its catalytic activity, we have undertaken structural and functional studies on SpAdK, and investigated the effect of SpAdK on pneumococcal growth.

*Abbreviations:* SpAdK, *Streptococcus pneumoniae* adenylate kinase; Ap5A, adenosine pentaphosphate

* Corresponding authors. Tel.: +82 31 290 5913; fax: +82 31 290 7015 (S. Lee). Tel.: +82 31 290 7707 (D.-K. Rhee).
*E-mail addresses:* sangholee@skku.edu (S. Lee), dkrhee@skku.edu (D.-K. Rhee).

[1] These two authors contributed equally.

http://dx.doi.org/10.1016/j.fob.2014.07.002
2211-5463/© 2014 The Authors. Published by Elsevier B.V. on behalf of the Federation of European Biochemical Societies.
This is an open access article under the CC BY-NC-ND license (http://creativecommons.org/licenses/by-nc-nd/3.0/).

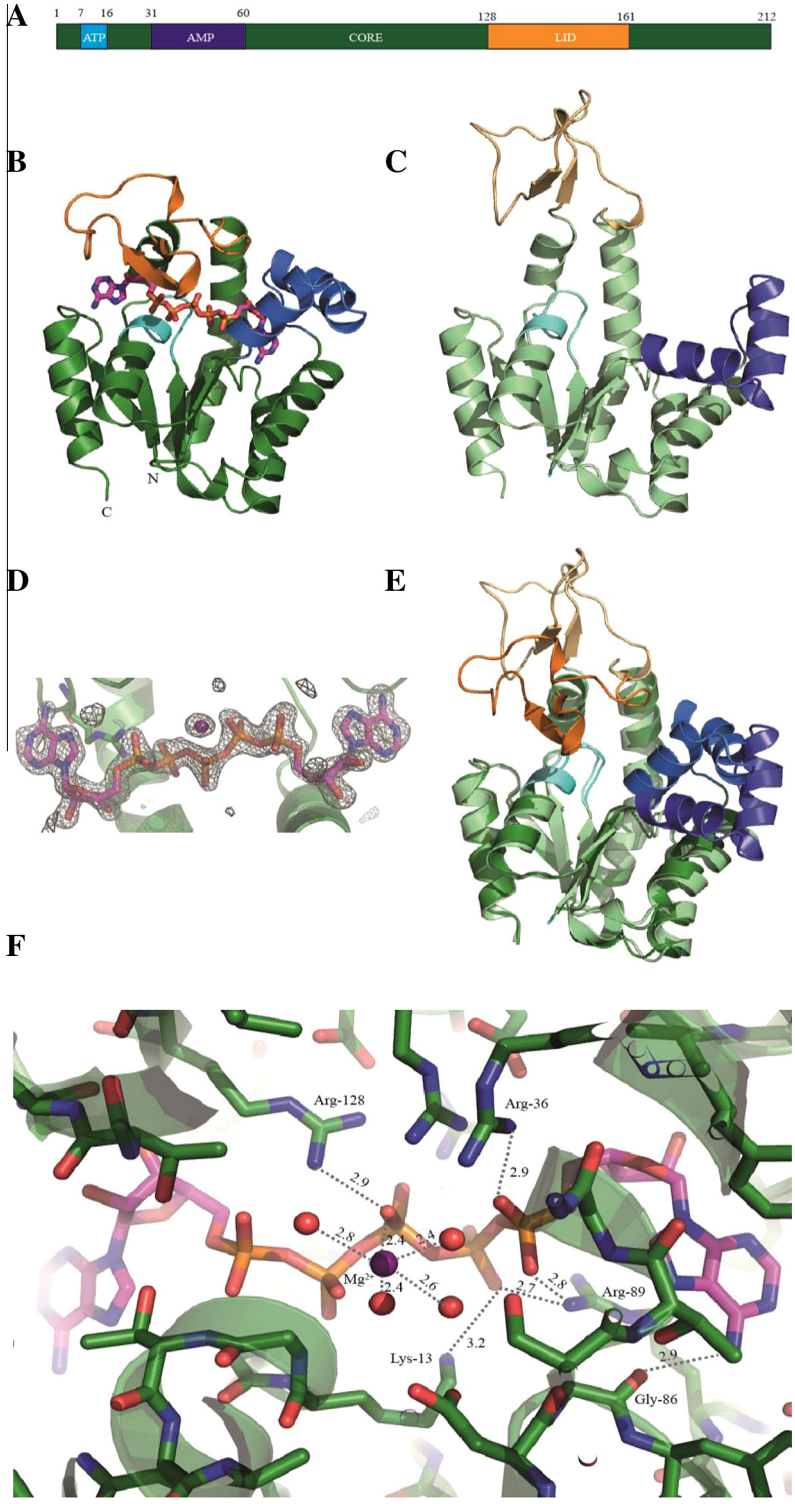


**Fig. 1.** Overview of SpAdK structure in two conformations. (A) SpAdK structure and its domains. (B) the crystal structure of SpAdK in complex with two mimic-substrates (Ap5A); the ATP, AMP, LID and CORE domains are colored with cyan, marine, orange and forest, respectively; Ap5A is shown by stick-view. (C) The crystal structure of native SpAdK, with ATP (light cyan), AMP (light blue), LID (light orange) and CORE (light green) domains. (D) The $2mF_o$-$DF_c$ electron density map at 1.48 A° resolution shows the Ap5A and cofactor $Mg^{2+}$ (magenta sphere). (E) Superposition of two structures. (F) An insight view of the two mimic-substrate-binding cleft, including $Mg^{2+}$ (magenta sphere), and 4 water molecules (red spheres). (For interpretation of the references to color in this figure legend, the reader is referred to the web version of this article.)

## 2. Results

### *2.1. Crystal structure of adenylate kinase from S. pneumoniae in two conformations*

SpAdK consists largely of core, nucleotide binding and lid domains (Fig. 1A). The nucleotide-binding domain is further divided into ATP and AMP binding domains. The crystal structures of SpAdK were determined in two conformations: inhibitor-bound closed form at 1.48 Å, and ligand-free, open form at 1.69 Å resolution (Fig. 1B and C). Both structures were deposited in the Protein Data Bank under the accession codes PDB: 4NU0 (closed structure with Ap5A) and PBD: 4NTZ (open structure).The overall folding of SpAdK features a typical α/β class structure, where α-helices wrap

around a central β-sheet region (Figs. 1B and C). The lid and core domains, as well as P-loop, form an ATP binding pocket; meanwhile, AMP binds to the pocket formed by the core and AMP domains. The lid and AMP domains can access the substrate-binding site in the open form, which is consistent with previous reports [10,11]. *P*1, *P*5-di(adenosine-5′) pentaphosphate (Ap5A), a two-substrate mimicking inhibitor, was well defined in the closed conformation (Fig. 1D). Structural comparison between the two conformations showed significant changes, in which both the lid and AMP domains move closer to the active site, allowing substrate access, in reference to the core domain (Fig. 1E). Superposition of each domain between the two conformations revealed that the lid domain shows the most variation, with 1.6 Å of r.m.s.d., supporting domain movement.

### 2.2. Structural comparison to known bacterial AdKs

The overall SpAdK structure is similar to those of other AdKs, with noticeable differences in the lid domain (Fig. 2). The superposition of open conformation structures from SpAdK, *E. coli* (*Ec*), *Aquifex aeolicus* (*Aa*), *Desulfovibrio gigas* (*Dg*), and *Homo sapiens* (*Hs*) using Dali server [12] showed significant differences in the higher mobile loops in the lid domain (Fig. 2A). For instance, the r.m.s.d. between Cα atoms from SpAdK and 4AKE (*E. coli*) structure is 3.2 Å. The number of residues in the lid domain is also different from other AdKs. Consistently, the sequence alignment from SpAdK and other AdKs shows the N-terminal region including P-loop (residues 7–16) is strictly conserved, whereas the lid domain and C-terminal region are variable (Fig. 2B). Interestingly, SpAdK does not contain a conserved metal-binding motif (Cys-X2-Cys-X16-Cys) in the lid domain [13].

### 2.3. Arg-89 is the most important residue for catalytic activity

The active site of SpAdK features several conserved Arg residues (Fig. 1F). The strictly conserved Arg-89 forms hydrogen bonds with oxygen atoms, in both the δ- and ε-phosphate group of Ap5A. The ε-phosphate group of Ap5A corresponds to the phosphate group of AMP. The hydrogen bond network among Arg-89, Glu-93, and Asp-61 is known to serve as a backbone in the catalysis and AMP domain rearrangements [14]. Moreover, Arg-89 is a part of the conserved G(Y/F)PR motif stabilizing AdK structure, and transferring a phosphate group from ATP to AMP [15]. Two other Arg residues, Arg-36 and Arg-128 form hydrogen bonds with oxygen atoms of the phosphate groups in Ap5A. Gly-86 recognizes adenine base of Ap5A, by forming hydrogen bond with N6β. Tyr-87 is roughly parallel to an adenine moiety of Ap5A, without apparent hydrogen bond formation. Magnesium ion is found to be coordinated by four water molecules, as well as oxygen atoms from the β- and γ-phosphate of Ap5A, in the active site of the closed SpAdK:Ap5A structure. Lys-13 is located in the P-loop, and known to form hydrogen bonds with oxygen atoms from the phosphate groups of ATP and AMP [15]. In our SpAdK:Ap5A structure, Nζ forms a hydrogen bond with oxygen atom from the δ-phosphate group of Ap5A (3.2 Å), but is a little bit distant from the O3γ of Ap5A (3.9 Å) for hydrogen bonding to occur.

To assess the catalytic roles of the active site residues, the catalytic activities of eight SpAdK mutated proteins were measured (Fig. 3). Since AdKs catalyze both ATP formation and hydrolysis [16], the catalytic activities of both directions were measured. Among the mutated proteins tested, mutation at Arg-89 most significantly deteriorated the activity. We tested both R89A and R89G, because previous studies suggested that mutating Arg to Ala or Gly was efficient, in reducing the catalytic activity [17,18]. For SpAdK, both R89A and R89G exhibited comparable reduction in activity. Since all the eight residues subject to mutagenesis were mutated to Ala, we used R89A for subsequent functional studies. Taken together, our results establish that Arg-89 is a critical residue for the catalytic activity of SpAdK.

### 2.4. SpAdK deficiency abolishes pneumococcal growth

To determine the role of SpAdK in pneumococcal growth, we generated *adk* mutant, in either serotype 2 encapsulated D39 (S type), or non-encapsulated CP1200 (R type). However, these *adk* mutant strains were not viable, implying that SpAdK protein is essential. Hence, we generated a fucose-inducible strain, which permits conditional expression of *adk* in *S. pneumoniae*. We fused a fucose promoter with the *adk* open reading frame, thus expressing *adk* gene only in the presence of fucose (Fig. 4 and Table 2). In *S. pneumoniae* D39, the *adk* gene (spd_0214) is flanked by upstream *secY* (spd_0213) and by downstream *infA* (spd_0215) genes. The 639 bp of the *adk* open reading frame is flanked by 150 bp and 118 bp intergenic regions at the 5′ and 3′ ends, respectively. Transcription of the *adk* is not affected by the upstream gene *secY* nor the erythromycin resistance cassette (*ermAM*) owing to the transcription terminators at up- and down-stream of the *adk* gene to prevent transcription from either end (Fig. 4A). A bacterial $\sigma^{70}$ promoter recognition program, *BPROM* [19], showed that putative promoters of the *secY*, *adk*, and *infA* genes are located in the upstream of these genes in the same orientation (Fig. 4B), suggesting that the *adk* and *infA* genes are transcribed independently. To confirm that fucose could regulate only *adk* transcription and not the flanking genes, total RNA was extracted in the presence of various concentrations of fucose and used for determination of mRNA level of the flanking genes by reverse transcription PCR (RT-PCR). RT-PCR data showed that *secY* and *ifnA* expression was not affected by fucose concentration (Fig. 4C), suggesting that fucose induces specifically *adk* expression but not its flanking genes and *adk* transcription does not affect expression of the flanking genes. Therefore, in our experimental system, *adk* was transcribed as a monocistronic.

We examined the effect of *adk* expression on pneumococcal growth using the aforementioned fucose-inducible expression system (Fig. 5). In the absence of L-(−)-fucose (fucose), pneumococcal growth was arrested. However, after supplementation of various concentrations of fucose into the culture, a good correlation between fucose concentration and level of the SpAdK was demonstrated (Fig. 5A). Higher fucose concentration gave rise to higher growth rate in the fucose-inducible strains, while the growth rates of both S (encapsulated) and R (non-encapsulated) wild-types (WTs) were not affected by the presence of fucose (Fig. 5B). At 0.1% fucose concentration where the expression level of *adk* is low, encapsulated D39 fucose-inducible *adk* strain (TTL01) showed lower growth rate (Fig. 5B-left), than the non-encapsulated CP1200 *adk* mutant (TTL04) (Fig. 5B-right). This observation implies that 0.1% fucose could generate enough ATP for R type mutant for growth, but not for S type mutant. We speculate that at 0.1% fucose, S type TTL01 could not produce enough ATP for growth, most likely due to the requirement of ATP for capsular polysaccharide synthesis. This result supports that SpAdK is essential for growth. Notably, SpAdK expression was also higher at log-phase, than the other phases (Fig. 5C), which supports the idea that SpAdK provides ATP for cellular activities. Supplementation of goat serum induced SpAdK level dose-dependently and pneumococcal growth (Fig. 5D), strongly implying the relationship between SpAdK expression and pneumococcal growth.

To further confirm the role of SpAdK in pneumococcal growth, pMV158 containing the WT *adk* gene or *adk*-R89A mutation was introduced into the *adk* inducible strains, and the requirement of SpAdK for growth was analyzed. When the WT *adk* gene was introduced into the *adk* inducible strains of S type (TTL01) and R type (TTL04), the resulting complemented strains (TTL02 and TTL05,

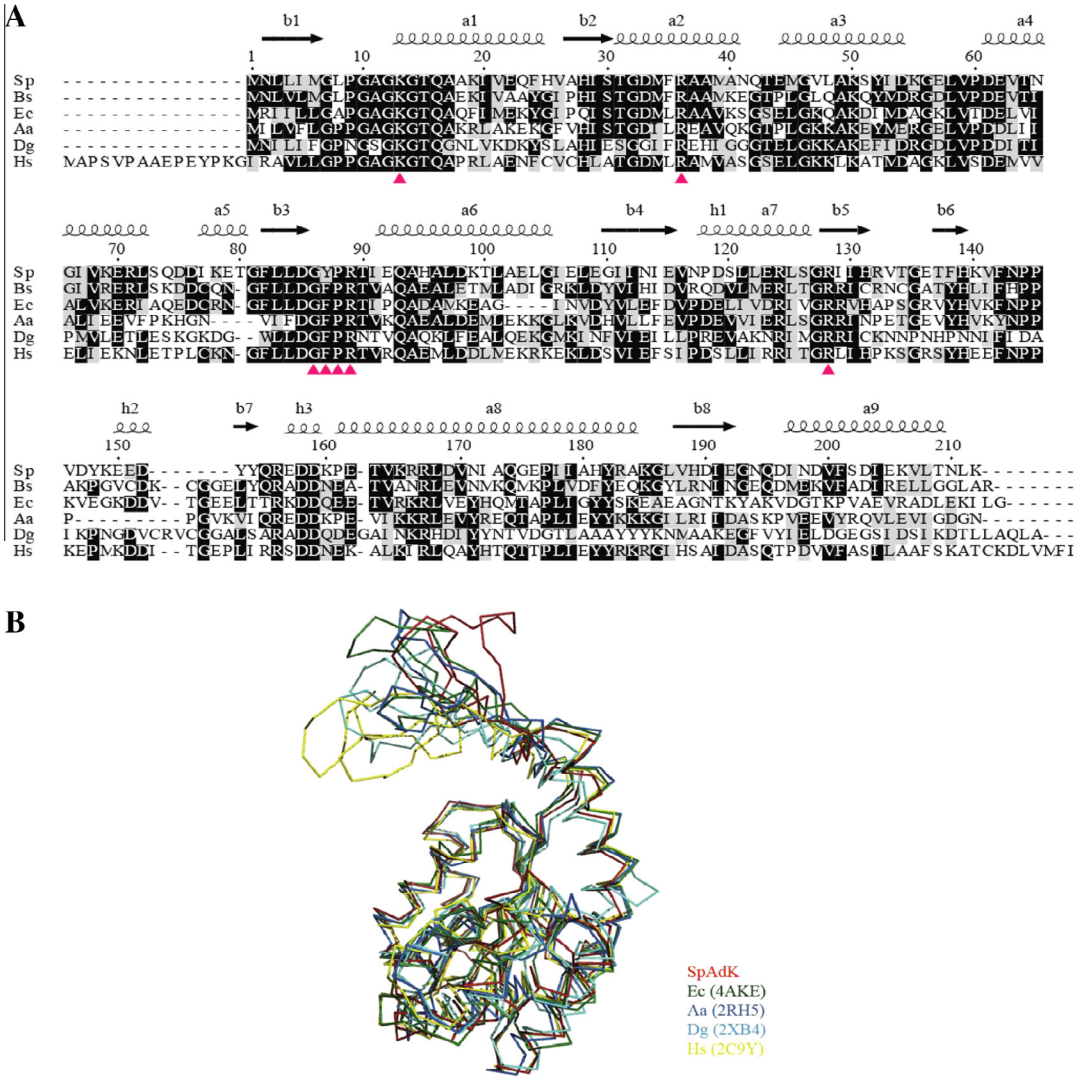


**Fig. 2.** (A) Secondary structure-based sequence alignment. (B) Structural superposition of SpAdK with AdKs from *Bacillus subtilis* (*Bs*), *Escherichia coli* (*Ec*); *Aquifex aeolicus* (*Aa*); *Desulfovibrio gigas* (*Dg*) and *Homo sapiens* (*Hs*). Conserved residues are labeled in black; arrows indicate the site-directed mutagenesis points.

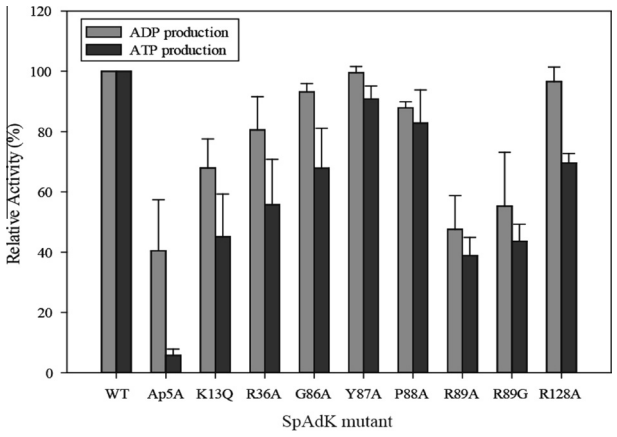


**Fig. 3.** Activity assay of SpAdK mutated proteins. ADP production assay (black bars) and ATP production assay (tilted gray bars) are shown. One-letter amino acid codes are used. Relative activities in reference to the wild type (WT) are shown.

respectively) resumed growth in the absence of fucose. In contrast, introduction of the R89A mutation to the *adk* inducible strains (TTL03 and TTL06) showed growth defect, and did not grow without fucose (Fig. 6). Collectively, these results demonstrate that SpAdK is essential for pneumococcal growth.

### 2.5. SpAdK increases intracellular ATP

Since AdK modulates ATP synthesis until ADP and ATP levels reach equilibrium, high concentration of fucose should produce high SpAdK activity, resulting in a higher level of ATP. Fucose was added into culture of the TTL01, and the intracellular ATP level was determined. At 1.0% fucose, the intracellular ATP level of the TTL01 strain was increased more than that of the D39 WT or TTL01 at 0.1% fucose, although the fucose itself did not affect the intracellular ATP level of the D39 WT (Fig. 7). These data consistently suggested that SpAdK is essential for ATP synthesis.

### 2.6. Lack of functional SpAdK attenuates pneumococcal growth in vivo

Since SpAdK plays an essential role in pneumococcal growth and ATP synthesis, role of SpAdK in virulence was determined *in vivo*. Prior to infection, the TTL01 strain was incubated in 0.5% fucose, and then administrated to mice via intranasal (*i.n.*) or intraperitoneal (*i.p.*) route ($1.5 \times 10^7$ CFU per mice). Results showed that the mice infected with the TTL01 survived much longer than

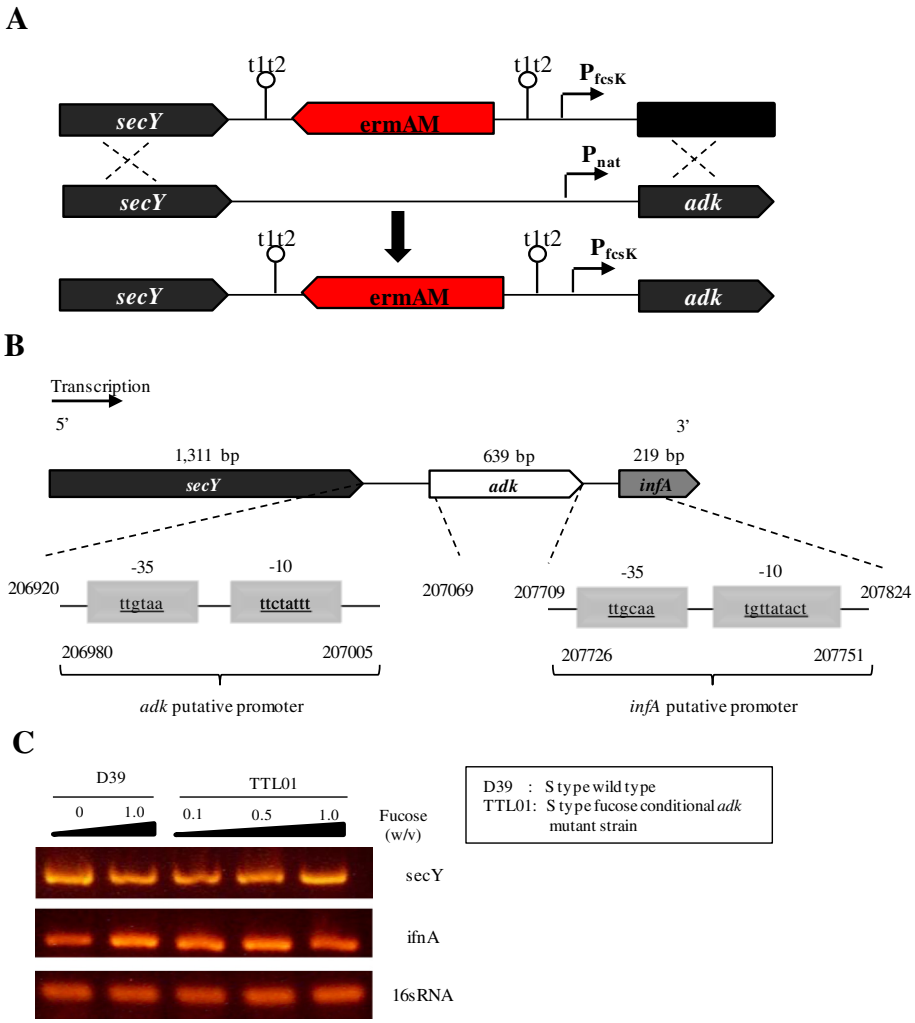


**Fig. 4.** Schematic of an inducible strain construction, *adk* locus and transcription. (A) Construction of *S. pneumoniae* type 2 *adk* fucose-inducible strain. (B) *adk* locus map. Putative promoters of *secY*, *adk*, and *infA* are found at the upstream region. Only putative promoters of *adk* and *infA* are shown. (C) mRNA level of the *secY* and *ifnA* genes was determined by RT-PCR analyses. Transcription of the *adk* flanking genes (*secY* and *ifnA* genes) was independent from the *adk* promoter.

the mice infected with the D39 WT, in both *i.p.* and *i.n.* infections (Fig. 8A). In particular, no mice were survived after infection *i.p.* with D39 WT at 30 h post-infection whereas all the mice were survived after infection with the TTL01. Consistently, 5 mice survived at 14 days post-infection once 14 were infected *i.n.* with D39 WT initially (5/14) while 13 survied once 15 were infected *i.n.* with the TTL01 (13/15). Moreover, a lower infection dose was also performed: after $1.5 \times 10^4$ CFU per mice *i.p.* and $1.5 \times 10^6$ CFU per mice *i.n.* infections, survival percentage of the mice infected with the TTL01, particularly 4/5 (80%) (*i.p.*) and 2/5 (40%) (*i.n.*), was also significantly higher than that of the mice infected with the WT demonstrating that the TTL01 mutant was unable to survive *in vivo* (Fig. 8B). Moreover, the number of viable cells of the TTL01 infection recovered from mice blood was $10^7$ and $10^8$-fold lower, than those of the D39 WT respectively (Fig. 8C), after *i.p.* and *i.n.* infections, indicating that the viability of the TTL01 is dramatically decreased, compared to that of the D39 WT, *in vivo*.

## 3. Discussion

ATP is a pivotal metabolic intermediate required for cell growth. Although AdK is not an ATP synthase, it reversely catalyzes two molecules of ADP to AMP and ATP. Since inactivation of AdK in *E. coli* decreased the rate of macromolecular synthesis [20], AdK seems to control cell growth via cellular energy homeostasis. However, the role of AdK of Gram-positive bacteria in normal growth has not been characterized yet. In this study, we found that an isogenic *adk* deletion mutant of *S. pneumoniae* was not viable. Thus, a conditional mutant using fucose inducible *adk* promoter was constructed, and correlationship between fucose concentration and growth rate was demonstrated. Moreover, dependence of pneumococcal growth on SpAdK was corroborated using complementation test and mutational studies with R89A (Figs. 5 and 6). Consistently, the fucose-dependent *adk* strain (TTL01) showed reduced viability *in vivo* (Fig. 8).

Although there are more than 90 serotypes of pneumococci, BLAST search results showed that strains of various serotypes show highly conserved *adk* sequence. The *adk* gene of the D39 strain (type 2) shares 100% homology with the R6 strain as well as serotypes 1 (INV104 and P1031 strains), 6B (670-6B), 15B (Netherlands15B-37), A19 (TCH8431), 19A (Hungary19A-6), 19F (Taiwan19F-14), and 23F (ATCC 700669), and 99% homology with serotypes 3 (OXC141 strain), 4 (TIGR4), 14 (INV200) and 19F (CGSP14 and G54), showing that *adk* gene is highly conserved across the serotypes of *S. pneumoniae*. From these results, it is understood that so long as it has high sequence homology between serotypes or strains of *S. pneumoniae*, the *adk* gene can be a useful target for inactivating or modulating the SpAdK activity to develop

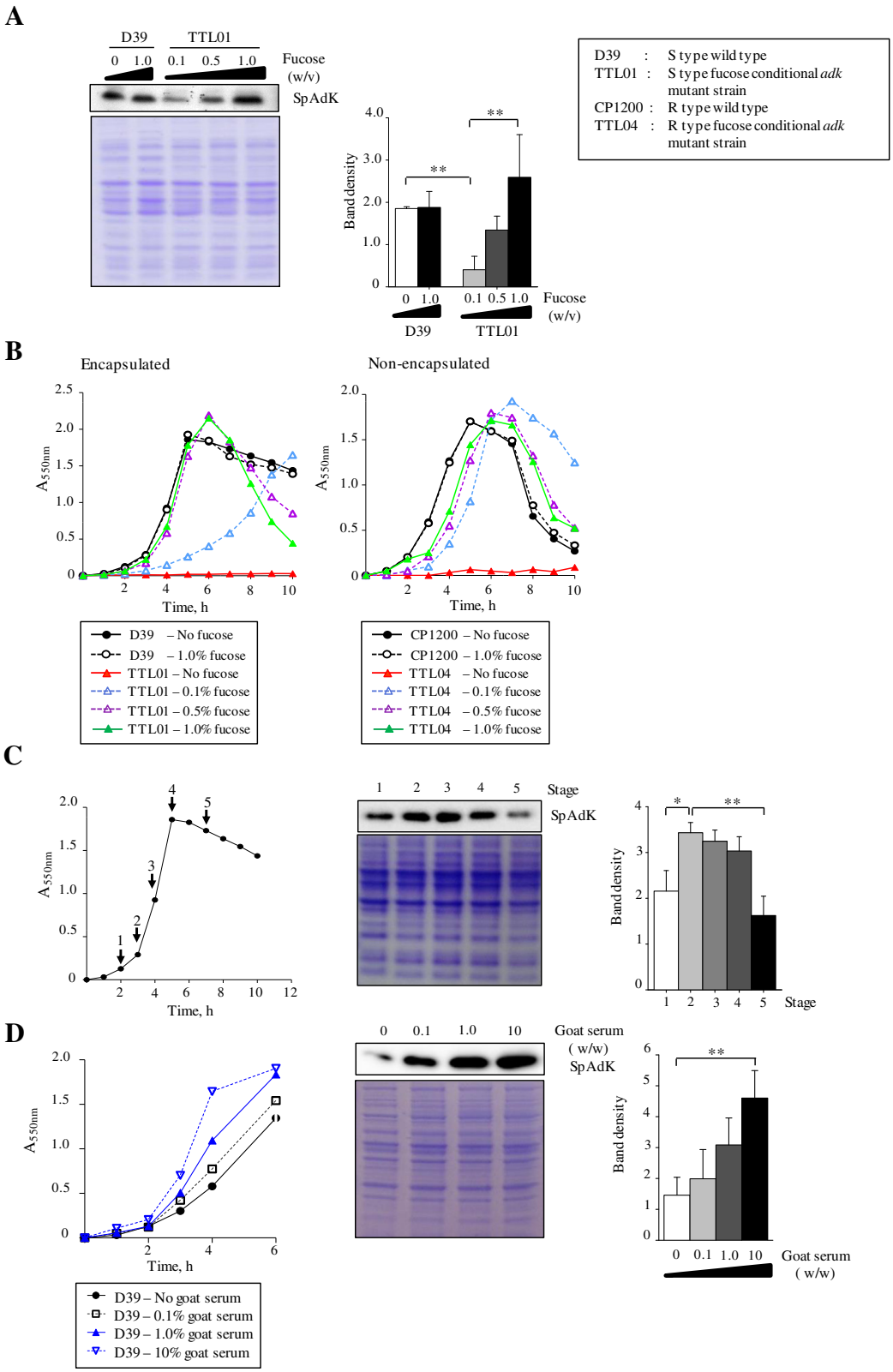


**Fig. 5.** Growth of fucose-inducible *adk* strain. (A) Fucose-dependent SpAdK induction in the TTL01, but not in D39 WT, at exponential phase. (B) Growth of D39 WT, TTL01 (left), and CP1200, TTL04 (right), in the presence of various fucose concentrations. (C) Growth-phase specific induction of SpAdK. (D) Dose-dependent induction of SpAdK by goat serum.

chemotherapeutic agents. So far 6 human AdK homologs are known: cytoplasmic AdK1 (GenBank ID: 4502011) and AdK5 (GeneBank ID: 257051028), and mitochondrial AdK2 (GenBank ID: 14424799), AdK3 (GenBank ID: 6518533), AdK4 (GeneBank ID: 125157), and nuclear AdK6 (GeneBank ID: 4507351) [21]. Except human AdK6, SpAdK is homologous to human AdKs at primary sequence level: 29%, 39%, 37%, 35%, and 29% sequence identity for AdK1, AdK2, AdK3, AdK4, and AdK5, respectively. Although

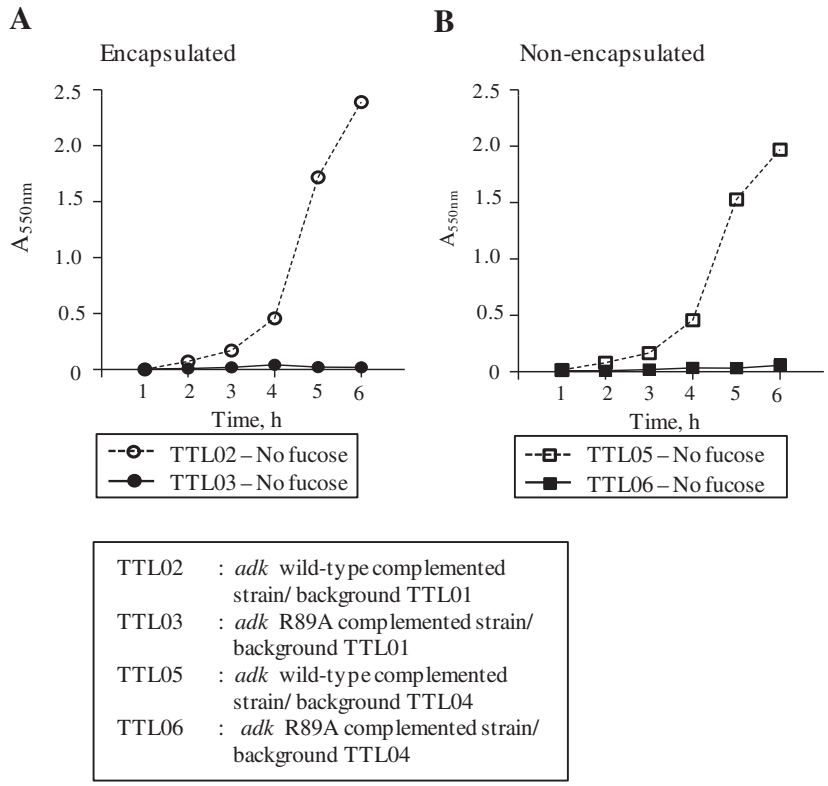


**Fig. 6.** Arg-89 of SpAdK is essential for growth. *S. pneumoniae adk* complemented strains (S type-TTL02 and R type-TTL05) grew in the absence of fucose whereas the strains comprising *adk*-R89A point-mutation strains (S type-TTL03 and R type-TTL06) did not grow.

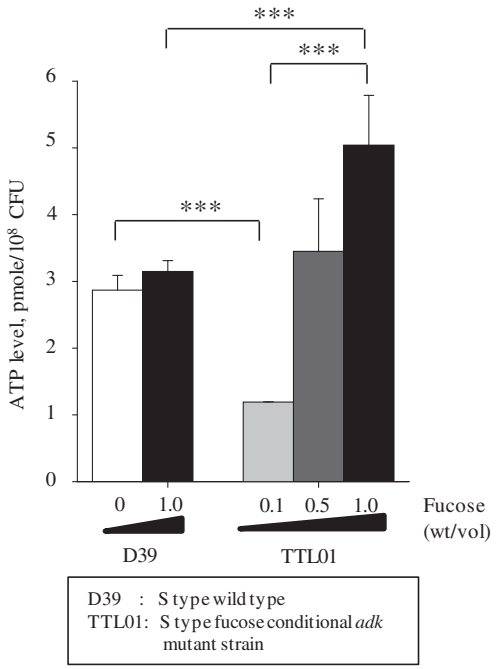


**Fig. 7.** SpAdK increases intracellular ATP. Total ATP levels in D39 and TTL01 (fucose-inducible *adk* mutant strain) are shown.

sequence identities of human AdK1–5 are not high, key catalytic residues and tertiary structure of human AdKs appear to be conserved as exemplified by human AdK2 (Fig. 2). Therefore, intervention of AdK activity for chemotherapeutics development should be based on allosteric modulation of SpAdK rather than direct interference with the active site.

AdK has been implicated in the pathogenesis in Gram-negative bacteria but not known in Gram-positive bacteria. For instance, AdK is secreted by the pathogenic Gram-negative strains of *Pseudomonas aeruginosa* and *Burkholderia cepacia* during infection and causes macrophage or mast cell death [7,22,23]. AdK secretion from pathogenic *B. cepacia* is specifically activated by eukaryotic protein α2-macroglobulin [22]. Pathogenic mucoid *P. aeruginosa* strains can increase the external ATP levels and kill macrophage via activation of P2Z receptor [23], which is responsible for pore formation on macrophage membrane [7,22,23]. Furthermore, at the site of inflammation, ATP concentration can be reached as high as hundreds micromolar [24], and ATP released by invading pathogens works as extracellular messengers and can be recognized readily by P2 receptors in innate immune cells. Although pneumococcal SpAdK was not secreted during infection (data not shown), our result does not rule out the possibility that pneumococcus would be lysed after invasion into the host cells resulting in release of SpAdK as well as nucleotides.

To adapt to hostile environments within the host, pathogenic bacteria can activate their virulence regulators via stringent signal responses mediated by guanosine 5′-diphosphate-3′-diphosphate (ppGpp) and guanosine 5′-triphosphate-3′-diphosphate ((p)ppGpp) [25]. The ppGpp mediates many physiological effects by direct or indirect control of transcription [25]. The ppGpp level in bacteria is modulated by both monofunctional synthetase RelA and bifunctional synthetase/hydrolase SpoT and RSH (RelA/SpoT homologue) proteins [25]. Both type of enzymes synthesize ppGpp from GDP or GTP, and by pyrophosphoryl transfer from ATP [26]. Most Gram-negative bacteria encode both RelA and SpoT whereas *S. pneumoniae*, a Gram-positive, encodes a bifunctional RSH protein $Rel_{Spn}$ and a RelA-like synthetase homologue RelQ. In enterohemorrhagic *E. coli*, accumulation of ppGpp by RelA induction leads to the increased gene expression in the locus of enterocyte efface-

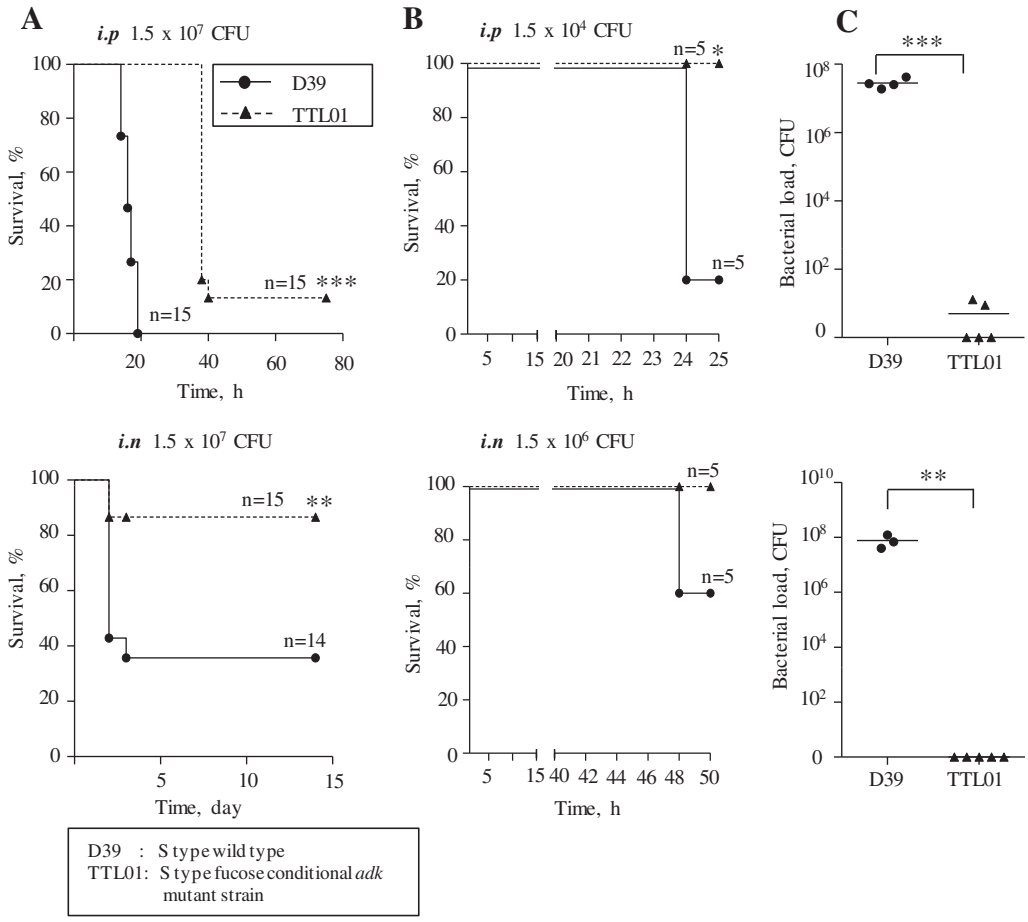


**Fig. 8.** (A) Attenuated virulence of the *adk* mutant *in vivo*. Groups of mice were infected *i.p.* or *i.n.* with approximately $1.5 \times 10^7$ CFU of D39 or TTL01 ($n$ = 14–15), and survival time was monitored for 80 h or 14 days for *i.p.* and *i.n.* infections, respectively. (B) Attenuated virulence of the *adk* mutant *in vivo* in low infection-dose, groups of mice were infected *i.p.* or *i.n.* with approximately $1.5 \times 10^4$ CFU or $1.5 \times 10^6$ CFU of D39 or TTL01 ($n$ = 5), and survival time was monitored for 24 h or 48 h for *i.p.* and *i.n.* infections, respectively. (C) Group of mice was infected *i.p.* with $1.5 \times 10^4$ or *i.n.* with $1.5 \times 10^6$ CFU of either D39 or TTL01 for 24 h (*i.p.*) or 48 h (*i.n.*), and number of viable bacteria in the blood was determined either 24 h (*i.p.*) or 48 h (*i.n.*) post infection after sacrifice, if they were alive, or post-mortem ($n$ = 3–5).

ment (LEE) by activation of virulence regulatory genes [27]. In *S. pneumoniae* type 2 D39, $Rel_{Spn}$ up-regulates the expression of pneumolysin (ply), a major pneumococcal virulence factor [28]. Since SpAdK regulates *S. pneumoniae* type 2 ATP level (Fig. 7) and ATP is pivotal for ppGpp metabolism, SpAdK might be involved in the pneumoccocal virulence. Therefore, further works on SpAdK virulence or cytotoxicity would warrant how SpAdK modulates cytotoxicity or virulence.

In this study, we investigated the structure and function of SpAdk, both *in vitro* and *in vivo*. We found SpAdK to be essential in pneumococcal growth. Cellular ATP levels increase in proportion to the SpAdK level, establishing that SpAdK is involved in energy homeostasis. The *adk* mutant showed defective growth *in vitro* and *in vivo*. Taken together, our results demonstrate that SpAdK is essential for pneumococcal growth.

## 4. Materials and methods

### 4.1. Cloning and mutagenesis

Gene encoding AdK in S. pneumoniae D39 (accession number, NC_008533.1) was amplified and inserted into parallel His2 parallel vector [29] between *Bam*HI and *Eco*RI restriction enzyme sites. All plasmids containing mutated sequences were generated using Quikchange II site-directed mutagenesis kit (Agilent Technologies), and then confirmed by DNA sequencing. *E. coli* strains were cultured in Luria Broth (LB) medium. Extraction and purification of plasmid DNAs from *E. coli* were performed using Qiagen kit (Qiagen).

### 4.2. Protein purification and crystallization

All proteins were expressed in *E. coli* BL21 (DE3) strain and purified by affinity chromatography on Ni–NTA resin (Qiagen). His-tag was cleaved using tobacco etch virus protease [30] by dialysis against buffer A (25 mM Tris–HCl pH 7.5, 75 mM NaCl, 1 mM $MgCl_2$ and 50 mM EDTA) overnight at 20 °C. The protein was further purified on Superdex-75 size exclusion column (GE Health-Care) equilibrated with buffer B (50 mM Tris–HCl pH 7.5, 150 mM NaCl, 1 mM $MgCl_2$). Fractions containing pure AdK were pooled and concentrated by 10 kDa-centrifugal filters (Ambicom). Protein monodispersity was checked by dynamic light scattering measurement on DynaPro 100 (Protein Solutions) in the buffer B.

Crystallization of SpAdK and SpAdK:Ap5A was attempted at 22 °C, by the hanging-drop vapor-diffusion method. SpAdK crystals were obtained by mixing 2.5 µl 18 mg/ml protein solution with 2.5 µl reservoir solution containing 2.0 M $(NH_4)_2SO_4$, 0.1 M CHES pH 9.5, 0.2 M $Li_2SO_4$, and 0.1 M $CsCl_2$. SpAdk:Ap5A crystals appeared in the reservoir containing 0.1 M sodium acetate, 0.1 M sodium acetate pH 4.6, 30% PEG 8 K, and 50 mM NaF. The crystals were transferred to a cryoprotectant solution containing 22.0 and 27.5% glycerol for SpAdK and SpAdK:Ap5A, respectively.

### 4.3. Data collection and structure determination

Diffraction data was collected at Photon Factory beamline BL-5A (Japan), SPring-8 beamline BL26B1 (Japan), and Pohang Accelerator Laboratory beamlines 5C and 7A (Korea). Data processing and reduction were carried out using *HKL2000* [31], *iMoslfm* [32] and *POINTLESS* [33] and *MOLPROBITY* [34]. Open, ligand-free SpAdK structure was solved by molecular replacement using *PHENIX* [35] with AdK from *Marinibacillus marinus* (PDB ID: 3FB4) and *Burkholderia pseudomallei* (PDB ID: 3GMT) as search models. Iterative manual model building and refinement were performed using *COOT* [36] and *PHENIX* [35]. The structure of SpAdK:Ap5A in closed conformation was solved by molecular replacement using open, ligand-free SpAdK structure as the search model. Statistics for data collection and structure refinement are shown in Table 1.

**Table 1**
Crystallographic data collection and refinement statistics.

| Conformation ligand | Closed Ap5A | Open |
|---|---|---|
| Data collection | | |
| Space group | *P*1 | $P2_1$ |
| Cell dimensions | | |
| *a*, *b*, *c* (Å) | 39.20, 48.34, 52.57 | 44.22, 53.7, 50.87 |
| *α*, *β*, *γ* (°) | 75.30, 72.95, 88.77 | 90, 114.46, 90 |
| Resolution (Å) | 1.48 (1.51–1.48)* | 1.70 (1.73 – 1.70) |
| $R_{r.i.m.}$[a] | 0.070 (0.304) | 0.093 (0.104) |
| $R_{p.i.m.}$[a] | 0.049 (0.215) | 0.051 (0.054) |
| $I/\sigma I$ | 25.27 (5.97) | 7.97 (6.80) |
| Completeness (%) | 93.11 (87.46) | 97.84 (98.72) |
| Redundancy | 3.7 (3.4) | 3.5 (3.4) |
| Refinement | | |
| Resolution (Å) | 50 – 1.48 | 25.05 – 1.69 |
| No. reflections | 54,770 | 23,924 |
| $R_{work}/R_{free}$ | 0.195/0.226 | 0.180/0.222 |
| No. atoms | 7,379 | 2,035 |
| Protein | 3,336 | 1,674 |
| Ligand/ion | 116 | 5 |
| Water | 583 | 356 |
| *B*-factors | 37.60 | 14.40 |
| Protein | 36.50 | 12.60 |
| Ligand/ion | | |
| Water | 46.00 | 22.80 |
| R.m.s. deviations | | |
| Bond lengths (Å) | 0.009 | 0.019 |
| Bond angles (°) | 1.39 | 1.79 |
| Ramachandran plot | | |
| Most favored regions (%) | 95.1 | 95.2 |
| Additional allowed regions (%) | 4.9 | 4.8 |

* Values in parentheses are for the highest-resolution shell.
[a] $R_{r.i.m.}$, redundancy-independent merging *R* factor; $R_{p.i.m.}$, precision-indicating merging *R* factor [45].

### 4.4. Activity assay

Enzymatic activity of SpAdK was determined by monitoring either ATP or ADP production. ATP production assay was performed in buffer C (25 mM phosphate pH 7.2, 5 mM $MgCl_2$, 65 mM KCl and 2 mM ADP). The buffer C was then preincubated at 37 °C for 5 min prior to the addition of SpAdK at the final concentration of 10 nM. The concentration of ATP was determined by following manufacturer's instruction of ATP determination kit (Invitrogen). ADP production from ATP and AMP was measured as described previously [37]. Briefly, the reaction buffer D for measuring ADP production contained 25 mM phosphate pH 7.2, 5 mM $MgCl_2$, 65 mM KCl, 0.12 mM NADH, 0.2 mM phosphoenolpyruvate, 10 units of both lactate dehydrogenase/pyruvate kinase mixture, 1.4 mM AMP and 50 μM ATP. ADP concentration was determined by subtracting the concentration of NADH consumed during the reaction from the NADH concentration of the control. All reagents for the assay were purchased from Sigma–Aldrich. Values shown are averaged ones from independent experiments in at least triplicate.

### 4.5. Bacterial strains conditions

The bacterial strains of *S. pneumoniae* and plasmids used in this study are shown in Table 2. Non-encapsulated *S. pneumoniae* CP1200, a derivative of Rx1 [38] or encapsulated *S. pneumoniae* D39 (serotype 2, NCTC7466) [39] was cultured in Casitone–tryptone-based medium (CAT) or Todd-Hewitt broth containing yeast extract (THY broth) as described previously [38,40]. Pneumococcal competence was controlled by appropriate addition of the competence stimulating peptide-1 as described previously [41]. Erythromycin (0.1 μg/ml) or tetracycline (1.0 μg/ml) was used to select pneumococcal transformants.

### 4.6. Construction of a fucose-inducible adk strain

A *S. pneumoniae* D39 fucose-inducible *adk* strain (D39 $P_{fcsK}$-*adk*; TTL01) was constructed by replacing *adk* promoter with the $P_{fcsK}$ inducible promoter in the chromosome of *S. pneumoniae* using a triple joining PCR amplification with overlapping primers (Table 3). First, a cassette containing an erythromycin resistance marker (*ermAM*), a fucose promoter ($P_{fcsK}$), and transcriptional terminators (t1,t2) that are located at the 5′ end of the $P_{fcsK}$ promoter was amplified from the Cheshire cassette, which was kindly provided by Morrison [42], using primers ermAM-F and ermAM-R [43]. Two arms were flanked by *S. pneumoniae* D39 DNA genome as follows: left arm contained a part of *secY* (upstream gene of *adk*) and ended at its stop codon, and was amplified by primers adk1 and adk2; right arm was initiated at *adk* start codon and forward 715 bp using primers adk3 and adk4. The cassette, left and right arms were used as templates for a triple-joining PCR using primers adk1 and adk4. The PCR product was integrated homogenously into *S. pneumoniae* D39 by transformation. The transformant was selected by 0.1 μg/ml erythromycin and 0.5% L-(−)-fucose (Sigma) and confirmed by sequencing.

### 4.7. RNA isolation and qRT-PCR

*S. pneumoniae* D39 and TTL01 were cultured to exponential phase prior to isolation of the RNA by hot phenol method as described previously [43]. One microgram of bacterial RNA was reverse transcribed into cDNA using a random primer (Takara) and MLV-RT enzyme (SUPER Bio). Quantitative reverse transcriptional PCR (qRT-PCR) was performed according to the manufacturer's instructions (Intron). Each condition was analyzed in triplicate.

### 4.8. Complementation test

For complementation test, *adk* wild-type or R89A mutant containing their natural promoters were inserted into pET28a vector (Novagen), then subcloned into pMV158 vector [43] by using *Hin*dIII and *Eco*RI restriction enzymes. The transformation of pMV158::*adk* and pMV158::*adk*-R89A into *S. pneumoniae* D39 *adk*-inducible strains were performed as previously described. The transformants were selected by 0.1 μg/ml erythromycin and 1.0 μg/ml tetracycline, and followed by colony PCR screening using tetracycline resistance-specific primers for pMV158. Transformants were selected and then used for plasmid isolation. Recombinant's nucleotide sequence was identified by PCR with adk_*Hin*dIII and adk_*Eco*RI primers and also confirmed by sequencing.

### 4.9. Pneumococcal ATP determination

*S. pneumoniae* was grown exponentially in THY with (0.1%, 0.5%, and 1.0%) or without fucose until $A_{550}$ = 0.5. Bacterial pellet was

**Table 2**
Pneumococcal strains and plasmids used in this study.

| Strains plasmids | Relevant characteristics | Antibiotic resistance | References |
|---|---|---|---|
| *Strains* | | | |
| D39 | Encapsulated, type 2 | | [39] |
| TTL01 | D39 $P_{fcsK}$::*adk* | ERY | This study |
| TTL02 | TTL01 containing pMV158-*adk* | ERY, TET | This study |
| TTL03 | TTL01 containing pMV158-*adk*-R89A | ERY, TET | This study |
| CP1200 | Non-encapsulated derivative of Rx1 *malM511-str1* | | [38] |
| TTL04 | CP1200 $P_{fcsK}$::*adk* | ERY | This study |
| TTL05 | TTL02 containing pMV15-*adk* | ERY, TET | This study |
| TTL06 | TTL02 containing pMV158-*adk*-R89A | ERY, TET | This study |
| *Plasmids* | | | |
| pMV158 | 5300 bp, streptococcal plasmid | TET | [43] |

**Table 3**
Primers used in this study.

| Name | Sequence (5′ → 3′) |
|---|---|
| adk1 | tac ctt ggc tgg agc tca at |
| adk2 | **tag gac tgc cta ccg aaa aa**t tat tct gtt ctg tcc atg a |
| adk3 | **gga cga aga gag aag aaa a**at gaa tct ttt gat tat ggg |
| adk4 | tcg att cga tcg ctc tag ac |
| ermAM-F | **ttt ttc ggt agg cag tcc ta**c cgt ggc tta ccg ttc gta tag |
| ermAM-R | **ttt tct tct ctc ttc gtc ctt ga** |
| adk_HindIII | ccc aag ctt atg aat ctt ttg att atg ggc tta |
| adk_EcoRI | cga att ctt att tca aat ttg tca ata ctt ttt |

lysed and used to determine ATP level as the instruction of ATP Determination Kit (Molecular Probes-Invitrogen). Quantitative determination of ATP in *S. pneumoniae* is based on recombinant firefly luciferase and L-luciferin reaction (luciferin + ATP + $O_2$ → oxyluciferin + AMP + pyrophosphate + $CO_2$ + light). Signals were detected via Luminometer (Tunner Biosystem) and ATP amount was quantified using an ATP standard curve.

### 4.10. Ethical statement for animal care and experiments

Male CD-1 (ICR) mice 4–5 weeks old (weighing approximately 20 g each, free-pathogens) were obtained from OrientBio Inc. (Seongnam, Korea), and acclimatized for a week. The animals were fed with water and sterile standard chow *ad libitum*. A specific pathogen-free barrier facility (12 h light/dark cycle, 22 ± 2 °C room temperature, 50 ± 10% relative humidity) at the School of Pharmacy at Sungkyunkwan University (Suwon, Korea) was used to maintain the animals. All animal experiments conformed to the animal care guidelines of the Korean Academy of Medical Sciences, and infection procedures followed protocol PH-530518-06 that was approved and monitored by the Animal Care and Use Committee of the Sungkyunkwan University (Suwon, Korea). For colonization experiment, mice were anesthetized using ketamine solution (80–100 mg/kg) prior to sacrifice for only blood collection.

For *in vivo* virulence test, mice ($n$ = 14–15) were infected either *i.n.* or *i.p.* with encapsulated D39 or its isogenic *adk* mutant TTL01 strain to evaluate effect of *adk* on pneumococcal survival and virulence. Prior to infection, pneumococci were cultured in THY broth in the presence of 0.5% or absence of fucose to approximately $A_{550}$ = 0.3 ($1.5 \times 10^8$ CFU/ml). Mouse was infected *i.n.* or *i.p.* with $1.5 \times 10^7$ CFU per mouse. The survival of mice was recorded within 80 h for *i.p.* infection or 14 days for *i.n.* infection. After infection, mice survival was monitored 8 times during first 4 days and 4 times until the end of the experiment.

To determine colonization of the bacteria, mice ($n$ = 5) were infected with $1.5 \times 10^4$ CFU *i.p.* or $1.5 \times 10^6$ CFU *i.n.* Mice were anesthetized using ketamine solution prior to sacrifice either at 24 h post-infection for *i.p.* infection or 48 h post-infection for *i.n.* infection [44]. Viable cells number in the blood was counted after serial dilution with phosphate buffer saline (PBS) prior to plating onto THY blood agar for D39 or agar supplemented with 0.5% (w/v) fucose and 0.1 μg/ml of erythromycin for TTL01.

### 4.11. Antisera and Western blot

Group of 5-week-old male CD1 mice ($n$ = 5) were immunized *i.p.* with 10 μg of purified SpAdK in combination with 100 μg of aluminum adjuvant (Sigma) at 14-day intervals. Mice were anesthetized using ketamine solution, and sera was collected from mice a week after the third immunization.

*S. pneumoniae* was grown exponentially in THY ($A_{550}$ = 0.5) and lysed in lysis buffer (50 mM Tris–Cl pH 8.0, 1 mM DTT, 0.1% Triton X-100, 1 mM protease inhibitor). Total proteins were collected and used for Western blot. Samples then were probed with appropriate antibody diluted 1:1000 fold in Tris buffer saline (TBS) containing 0.1% Tween20 (Sigma). The secondary antibody was anti-mouse or anti-rabbit immunoglobulin G conjugated with horse radish peroxidase (HRP) diluted 1:10,000 fold with TBS containing 0.1% Tween20 (Sigma).

### 4.12. Statistical analyses

Most of the graphs and statistical analyses were prepared using SigmaPlot 11.0 software (Systat Software), except *in vivo* tests (Fig. 8), which were prepared using GraphPad Prism version 5.02. Statistical analysis was calculated using an appropriate One Way ANOVA (Duncan's method, non-parametric), Student's *t*-test (non-parametric), Mann Whitney *U* Test (non-parametric), or Log-rank Test. A value of $P \leqslant 0.05$ (denoted by $^{*}$), $P \leqslant 0.01$ (denoted by $^{**}$) and $P \leqslant 0.001$ (denoted by $^{***}$), was considered significant. Data presented are the mean SD of the mean for 2–4 independent experiments.

## Author contribution

Planned the experiments: DR SL. Performed the experiments: TT, TL. Analyzed the data: TT TL SL DR. Wrote the paper: TT TL SL DR.

## Acknowledgements

We thank the beamline staff members at Photon Factory, SPring-8 and Pohang Accelerator Laboratory. We also acknowledge Dr. Donald Morrison for his donation of a Cheshire cassette and other vectors, for construction of the L-fucose-regulated strain. This work was supported by the Basic Science Research Program, through the National Research Foundation of Korea (NRF), funded by the Ministry of Education, Science, and Technology (NRF-2013R1A1A2059981 to S.L. and 2011-0024794 to D.R.), the Pioneer Research Center Program (2012-0009597) through the National

Research Foundation of Korea (NRF), and the Woo Jang Chun Program (PJ009106) through the Rural Development Agency to S.L., and by the Korea Science & Engineering Foundation (WCU R33-10045) to D.R.

## Appendix A. Supplementary data

Supplementary data associated with this article can be found, in the online version, at http://dx.doi.org/10.1016/j.fob.2014.07.002.

## References


[1] Liu, L., Johnson, H.L., Cousens, S., Perin, J., Scott, S., Lawn, J.E., Rudan, I., Campbell, H., Cibulskis, R., Li, M., Mathers, C. and Black, R.E. (2012) Global, regional, and national causes of child mortality: an updated systematic analysis for 2010 with time trends since 2000. Lancet 379, 2151–2161.

[2] Mitchell, A.M. and Mitchell, T.J. (2010) *Streptococcus pneumoniae*: virulence factors and variation. Clin. Microbiol. Infect. 16, 411–418.

[3] Lee, E.-J. and Groisman, E.A. (2012) Control of a *Salmonella virulence* locus by an ATP-sensing leader messenger RNA. Nature 486, 271–275.

[4] Atkinson, A. (1968) The energy charge of the adenylate pool as a regulatory parameter. Interaction with feedback modifiers. Biochemistry 7, 4030–4034.

[5] Chapman, A.G., Fall, L. and Atkinson, D.E. (1971) Adenylate energy charge in *Escherichia coli* during growth and starvation. J. Bacteriol. 108, 1072–1086.

[6] Jacobs, A., Didone, L., Jobson, J., Sofia, M., Krysan, D. and Dunman, P. (2013) Adenylate kinase release as a high-throughput-screening-compatible reporter of bacterial lysis for identification of antibacterial agents. Antimicrob. Agents Chemother. 51, 26.

[7] Markaryan, A., Zaborina, O., Punj, V. and Chakrabarty, A.M. (2001) Adenylate kinase as a virulence factor of *Pseudomonas aeruginosa*. J. Bacteriol. 183, 3345–3352.

[8] Dzeja, P. and Terzic, A. (2009) Adenylate kinase and AMP signaling networks: metabolic monitoring, signal communication and body energy sensing. Int. J. Mol. Sci. 10, 1729–1772.

[9] Haase, G.H.W., Brune, M., Reinstein, J., Pai, E.F., Pingoud, A. and Wittinghofer, A. (1989) Adenylate kinases from thermosensitive *Escherichia coli* strains. J. Mol. Biol. 207, 151–162.

[10] Muller, C.E. and Schulz, G.E. (1992) Structure of the complex between adenylate kinase from *Escherichia coli* and the inhibitor Ap5A refined at 1.9 A resolution. A model for a catalytic transition state. J. Mol. Biol. 224, 159–177.

[11] Henzler-Wildman, K.A., Vu, T., Lei, M., Ott, M., Wolf-Watz, M., Fenn, T., Pozharski, E., Wilson, M.A., Petsko, G.A., Karplus, M., Hübner, C.G. and Kern, D. (2007) Intrinsic motions along an enzymatic reaction trajectory. Nature 450, 838–844.

[12] Holm, L. and ROsenstrom, P. (2010) Dali server: conservation mapping in 3D. Nucleic Acids Res. 38, W545–W549.

[13] Bae, E. and Phillips, G.N. (2004) Structures and analysis of highly homologous psychrophilic, mesophilic, and thermophilic adenylate kinases. J. Biol. Chem. 279, 28202–28208.

[14] Krishnamurthy, H., Lou, H., Kimple, A., Vieille, C. and Cukier, R.I. (2005) Associative mechanism for phosphoryl transfer: a molecular dynamics simulation of *Escherichia coli* adenylate kinase complexed with its substrates. Proteins 50, 88–100.

[15] Bellinzoni, M., Haouz, A., Graña, M., Munier-Lehmann, H., Shepard, W. and Alzari, P. (2006) The crystal structure of *Mycobacterium tuberculosis* adenylate kinase in complex with two molecules of ADP and $Mg^{2+}$ supports an associative mechanism for phosphoryl transfer. Protein Sci. 15, 1489–1493.

[16] Huss, R.J. and Glaser, M. (1983) Identification and purification of an adenylate kinase-associated protein that influences the thermolability of adenylate kinase from a temperature-sensitive adk mutant of *Escherichia coli*. J. Biol. Chem. 258, 13370–13376.

[17] Reinstein, J., Gilles, A.-M., Rose, T., Wittinghofer, A., Girons, I.S., Barzu, O., Surewicz, W.K. and Mantsch, H.H. (1989) Structural and catalytic role of Arginine 88 in *Escherichia coli* adenylate kinase as evidenced by chemical modification and site-directed mutagenesis. J. Biol. Chem. 264, 8107–8112.

[18] Kim, H.J., Nishikawa, S., Tokutomi, Y., Takenaka, H., Hamada, M., Kuby, S.A. and Uesugi, S. (1990) In vitro mutagenesis studies at the arginine residues of adenylate kinase. A revised binding site for AMP in the X-ray-deduced model. Biochemistry 29, 1107–1111.

[19] Bitoun, J.P., Liao, S., Yao, X., Xie, G.G. and Wen, Z.T. (2012) The Redox-sensing regulator Rex modulates central carbon metabolism, stress tolerance response and Biofilm formation by *Streptococcus mutans*. PLoS One 7, e44766.

[20] Chakrabarty, A.M. (1998) Nucleoside diphosphate kinase: role in bacterial growth, virulence, cell signalling and polysaccharide synthesis. Mol. Microbiol. 28, 875–882.

[21] Drakou, C.E., Malekkou, A., Hayes, J.M., Lederer, C.W., Leonidas, D.D., Oikonomakos, N.G., Lamond, A.I., Santama, N. and Zographos, S.E. (2012) HCINAP is an atypical mammalian nuclear adenylate kinase with an ATPase motif: structural and functional studies. Proteins 80, 206–220.

[22] Melnikov, A., Zaborina, O., Dhiman, N., Prabhakar, B.S., Chakrabarty, A.M. and Hendrickson, W. (2000) Clinical and environmental isolates of *Burkholderia cepacia* exhibit differential cytotoxicity towards macrophages and mast cells. Mol. Microbiol. 36, 1481–1493.

[23] Zaborina, O., Misra, N., Kostal, J., Kamath, S., Kapatral, V., El-Idrissi, M.E.-A., Prabhakar, B.S. and Chakrabarty, A.M. (1999) P2Z-independent and P2Z receptor-mediated macrophage killing by *Pseudomonas aeruginosa* isolated from cystic fibrosis patients. Infect. Immun. 67, 5231–5242.

[24] Weber, F.C., Esser, P.R., Müller, T., Ganesan, J., Pellegatti, P., Simon, M.M., Zeiser, R., Idzko, M., Jakob, T. and Martin, S.F. (2010) Lack of the purinergic receptor P2X7 results in resistance to contact hypersensitivity. J. Exp. Med. 207, 2609–2619.

[25] Dalebroux, Z.D., Svensson, S.L., Gaynor, E.C. and Swanson, M.S. (2010) PpGpp conjures bacterial virulence. Microbiol. Mol. Biol. Rev. 74, 171–199.

[26] Potrykus, K. and Cashel, M. (2008) (p)ppGpp: still magical?∗. Annu. Rev. Microbiol. 62, 35–51.

[27] Nakanishi, N., Abe, H., Ogura, Y., Hayashi, T., Tashiro, K., Kuhara, S., Sugimoto, N. and Tobe, T. (2006) PpGpp with DksA controls gene expression in the locus of enterocyte effacement (LEE) pathogenicity island of enterohaemorrhagic *Escherichia coli* through activation of two virulence regulatory genes. Mol. Microbiol. 61, 194–205.

[28] Kazmierczak, K.M., Wayne, K.J., Rechtsteiner, A. and Winkler, M.E. (2009) Roles of relSpn in stringent response, global regulation and virulence of serotype 2 *Streptococcus pneumoniae* D39. Mol. Microbiol. 72, 590–611.

[29] Sheffield, P., Garrard, S. and Derewenda, Z. (1999) Overcoming expression and purification problems of RhoGDI using a family of "parallel" expression vectors. Protein Expr. Purif. 15, 34–39.

[30] Oldenburg, P.J., Wyatt, T.A., Factor, P.H. and Sisson, J.H. (2008) Alcohol feeding blocks methacholine-induced airway responsiveness in mice. Am. J. Physiol. Lung Cell. Mol. Physiol. 296, L109–L114.

[31] Kareyeva, A.V., Grivennikova, V.G., Cecchini, G. and Vinogradov, A.D. (2011) Molecular identification of the enzyme responsible for the mitochondrial NADH-supported ammonium-dependent hydrogen peroxide production. FEBS Lett. 585, 385–389.

[32] Battye, T.G., Kontogiannis, L., Johnson, O., Powell, H.R. and Leslie, A.G. (2011) IMOSFLM: a new graphical interface for diffraction-image processing with MOSFLM. Acta Crystallogr. D Biol. Crystallogr. 67, 271–281.

[33] Evans, P. (2006) Scaling and assessment of data quality. Acta Crystallogr. D Biol. Crystallogr. 62, 72–82.

[34] Chen, V.B., Arendall 3rd, W.B., Headd, J.J., Keedy, D.A., Immormino, R.M., Kapral, G.J., Murray, L.W., Richardson, J.S. and Richardson, D.C. (2010) MolProbity: all-atom structure validation for macromolecular crystallography. Acta Crystallogr. D Biol. Crystallogr. 66, 12–21.

[35] Murshudov, G.N., Vagin, A.A. and Dodson, E.J. (1997) Refinement of macromolecular structures by the maximum-likelihood method. Acta Crystallogr. D Biol. Crystallogr. 53, 240–255.

[36] Emsley, P. and Cowtan, K. (2004) Coot: model-building tools for molecular graphics. Acta Crystallogr. D Biol. Crystallogr. 60, 2126–2132.

[37] Davlieva, M. and Shamoo, Y. (2009) Structure and biochemical characterization of an adenylate kinase originating from the psychrophilic organism *Marinibacillus marinus*. Acta Crystallogr. Sect. F Struct. Biol. Cryst. Commun. 65, 751–756.

[38] Choi, I.H., Shim, J.H., Kim, S.W., Kim, S.N., Pyo, S.N. and Rhee, D.K. (1999) Limited stress response in *Streptococcus pneumoniae*. Microbiol. Immunol. 43, 807–812.

[39] Avery, O.T., MacLeod, C.M. and McCarty, M. (1944) Studies on the chemical nature of the substance inducing transformation of pneumococcal types induction of transformation by a desoxyribonucleic acid fraction isolated from pneumococcus type III. J. Exp. Med. 79, 137–158.

[40] Kwon, H.-Y., Kim, S.-W., Choi, M.-H., Ogunniyi, A.D., Paton, J.C., Park, S.-H., Pyo, S.-N. and Rhee, D.-K. (2003) Effect of heat shock and mutations in ClpL and ClpP on virulence gene expression in *Streptococcus pneumoniae*. Infect. Immun. 71, 3757–3765.

[41] Bricker, A.L. and Camilli, A. (1999) Transformation of a type 4 encapsulated strain of *Streptococcus pneumoniae*. FEMS Microbiol. Lett. 172, 131–135.

[42] Weng, L., Biswas, I. and Morrison, D.A. (2009) A self-deleting Cre–lox–ermAM cassette, Cheshire, for marker-less gene deletion in Streptococcus pneumoniae. J. Microbiol. Methods 79, 353–357.

[43] Tran, T.D.-H., Kwon, H.-Y., Kim, E.-H., Kim, K.-W., Briles, D.E., Pyo, S. and Rhee, D.-K. (2011) Decrease in penicillin susceptibility due to heat shock protein ClpL in *Streptococcus pneumoniae*. Antimicrob. Agents Chemother. 55, 2714–2728.

[44] Stroeher, U.H., Paton, A.W., Ogunniyi, A.D. and Paton, J.C. (2003) Mutation of luxS of *Streptococcus pneumoniae* affects virulence in a mouse model. Infect. Immun. 71, 3206–3212.

[45] Weiss, M.S. (2001) Global indicators of X-ray data quality. J. Appl. Cryst. 34, 130–135.